

Systematic Approach for Structure Elucidation of Polyphenolic Compounds Using a Bottom-up Approach Combining Ion Trap Experiments and Accurate Mass Measurements

Christoph von Bargaen, Florian Hübner, Benedikt Cramer, Sebastian Rzeppa, and Hans-Ulrich Humpf*

Institute of Food Chemistry, Westfälische Wilhelms-Universität Münster, Corrensstrasse 45, 48149 Münster, Germany

S Supporting Information

ABSTRACT: Polyphenols are a group of plant secondary metabolites with a wide range of structural differences. In many cases, *in vitro* and *in vivo* studies of polyphenols revealed beneficial health effects. The mass spectrometric characterization of polyphenols can be the key to understanding the metabolism and resorption of this group of substances. For structure elucidation of polyphenolic compounds nuclear magnetic resonance spectroscopy is the method of choice. Due to the broad structure variability and the sometimes relatively low concentrations of polyphenols and/or their metabolites in foods as well as physiological samples, mass spectrometry could be an alternative for structure elucidation. Especially high-resolution mass spectrometry, for example, Fourier transformation mass spectrometry (FTMS), is a valuable tool. Using a FTMS system, a systematic approach to the fragmentation behavior of phenolic and polyphenolic compounds was chosen to verify the influence of the structure on the fragmentation pattern of the different substances. Depending on the structure, specific fragment ions could be detected. Therefore, it is possible to gain reliable information about the structure of the pseudomolecular ion from its fragmentation spectrum, which is of great aid in the structure elucidation of unknown polyphenols and/or their metabolites.

KEYWORDS: polyphenols, structure elucidation, mass spectrometry, fragmentation, Fourier transformation mass spectrometry (FTMS), high-resolution mass spectrometry (HRMS)

INTRODUCTION

Polyphenols are among the most common plant secondary metabolites. An important group of polyphenols are the condensed tannins, also known as proanthocyanidins (PA). They can be found in many fruits,¹ nuts, and cereals^{2,3} and are therefore part of the human diet. A subgroup of the PA are the procyanidins (PC), with catechin and epicatechin as building units. In Figure 1 are shown the substances used in this study. They range from oligomeric to polymeric compounds built of flavan-3-ol units linked through C–C linkage (B-type PC) and more seldom through an additional ether bond (A-type PC). The C–C linkage is usually between C4 and C8 but can also be between C4 and C6.⁴

In food PC contribute to a bitter and astringent taste. Besides this, many beneficial health effects of PA and PC have been described in the literature. Studies showed antioxidative^{5,6} and chemoprotective effects against cancer.⁷ Further studies also showed a protective effect against cardiovascular diseases.⁸ Another interesting effect of PC is the ability to interact with proteins in the human body, for example, saliva proteins.⁹

However, as most effects are currently only observed *in vitro*, recent publications are more focused on the resorption and metabolism in the intestinal system in advanced model systems and *in vivo*.^{10,11} In these studies new metabolites are often detected, but due to the small amounts they are only poorly characterized. Nevertheless, structure elucidation of these PA and their metabolites is an essential part of understanding their mode of action. Usually NMR spectroscopy is the preferred method for structure elucidation as it enables the determination of not only the structure of a compound but also the

stereochemistry. Even though it is not possible to determine the stereochemistry of a compound with mass spectrometry (MS), it provides some advantages as it needs a far smaller amount of the unknown substance for analysis and impurities of the sample do usually not disturb the MS experiments. Due to the low amounts of PA and metabolites to be found under physiological conditions, structure elucidation with nuclear magnetic resonance spectroscopy (NMR), as the preferred method, is not possible. Therefore, mass spectrometry based fragmentation of molecules is a powerful method for structure elucidation.

In the literature the most commonly used system is liquid chromatography/electrospray ionization tandem mass spectrometry (LC/ESI-MS-MS). Another system is the LC/ESI coupled to an iontrap combined with an exact mass detector, for example, Thermo Scientific's LTQ Orbitrap XL (FTMS). Especially with the accurate mass in combination with fragmentation experiments it is possible to identify unknown compounds in plant samples and unknown metabolites in physiological samples.¹²

Analysis of reference substances with known structure gives distinctive fragmentation patterns, which are crucial for structure elucidation of unknown compounds.¹³ Further attempts in this direction have been recently performed by van der Hooff et al.¹⁴ This group used FTMS data to create and

Received: July 12, 2012

Revised: October 25, 2012

Accepted: October 26, 2012

Published: October 26, 2012

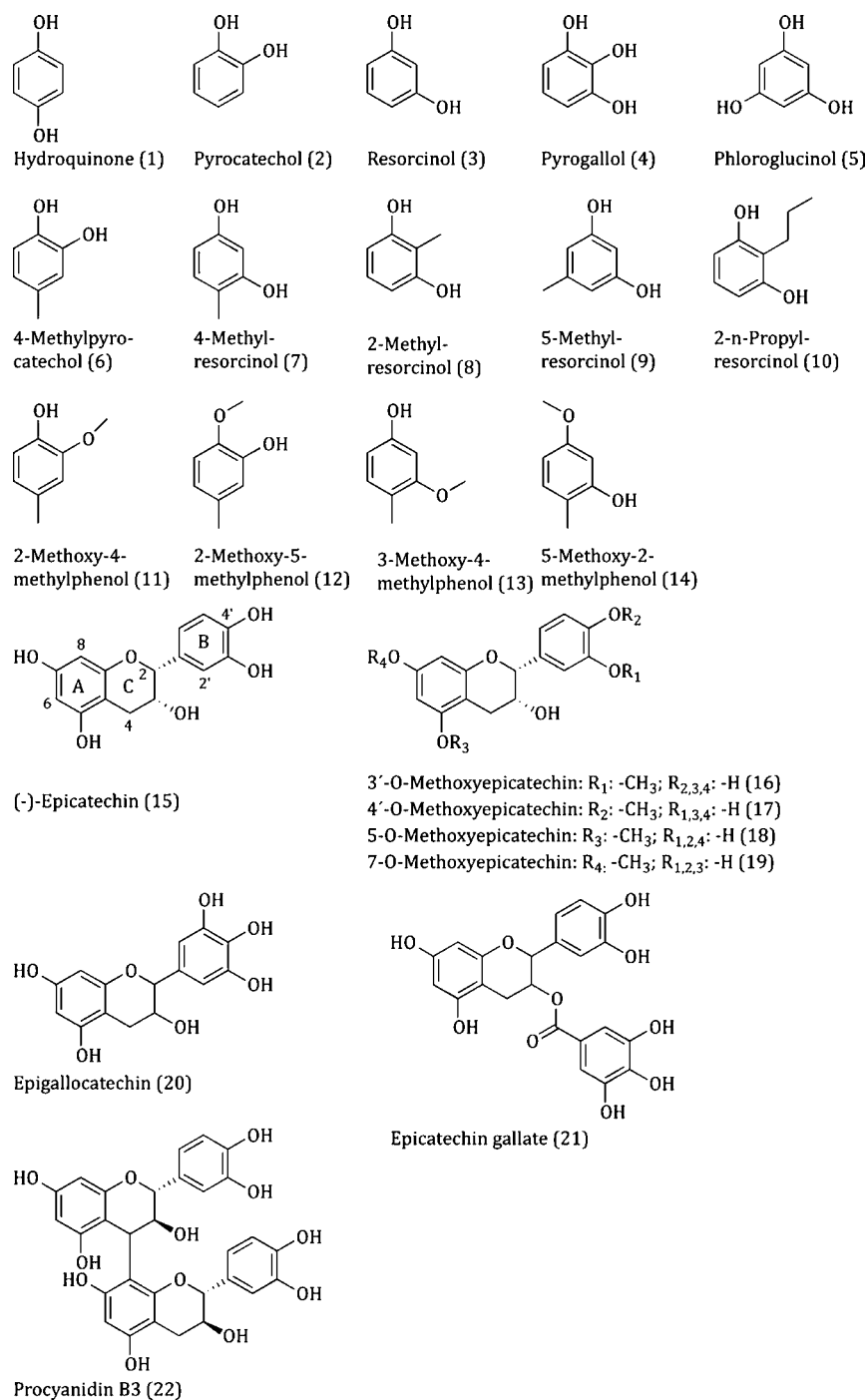


Figure 1. Structures of phenolic compounds (1–22) used in this study.

compare spectral trees of several compounds, for example, quercetin, several methoxyflavonols, and their glucosides. In their study, van der Hoof et al. also checked if the change of collision energy or concentration of the compound has an influence on the intensities of fragment ions. In both cases they observed only minor effects. They also compared the influence of the hydroxylation pattern, for example, of morin and quercetin, on the fragmentation behavior.¹⁴

In the present work 22 phenolic compounds (Figure 1) have been analyzed in MSⁿ experiments using FTMS with electrospray ionization (ESI) in the negative mode. The generated comprehensive fragmentation patterns were then used to describe fragmentation pathways based on published

reaction mechanisms. Starting with small phenolic compounds, coherencies between specific substructures in the molecules and characteristic fragmentation pattern were observed, allowing the assignment of substructures of larger PCs.

■ MATERIALS AND METHODS

Resorcinol (CAS Registry No. 108-46-3), brenzcatechin (CAS Registry No. 120-80-9), hydroquinone (CAS Registry No. 123-31-9), phloroglucinol (CAS Registry No. 108-73-6), pyrogallol (CAS Registry No. 87-66-1), and 4-methylpyrocatechol (CAS Registry No. 452-86-8) were purchased from Merck Schuchardt (Hohenbrunn, Germany); 4-methylresorcinol (CAS Registry No. 496-73-1) and 5-methylresorcinol (CAS Registry No. 504-15-4) were purchased from

Table 1. FTMS Parameters Used To Analyze Substances 1–21

substance	source voltage (kV)	vaporizer temp (°C)	sheath gas flow rate (arb)	aux gas flow rate (arb)	capillary voltage (V)	capillary temp (°C)	tube lens voltage (V)	CID	isolation width
1	3.5	155	7	5	-14	175	-64	45	1.20
2	3.0	155	7	5	-14	175	-64	45	1.20
3	3.5	155	7	5	-14	175	-64	45	1.20
4	3.0	55	7	5	-2	225	-89	45	1.20
5	3.0	55	7	5	-2	225	-89	45	1.20
6	3.5	155	7	5	-26	175	-99	50	1.20
7	3.5	155	7	5	-26	175	-99	50	1.20
8	3.5	155	7	5	-26	175	-99	50	1.20
9	3.5	155	7	5	-26	175	-99	50	1.20
10	3.5	155	7	5	-27	175	-89	55	1.20
11	3.5	155	7	5	-34	175	-64	45	1.20
12	3.5	155	7	5	-34	175	-64	45	1.20
13	3.5	155	7	5	-34	175	-64	45	1.20
14	3.5	155	7	5	-34	175	-64	45	1.20
15	3.3	55	8	5	-22	225	-104	25	1.20
16	3.0	53	7	5	-22	225	-104	18	1.20
17	3.0	53	7	5	-22	225	-104	18	1.20
18	3.0	53	7	5	-22	225	-104	18	1.20
19	3.0	53	7	5	-22	225	-104	18	1.20
20	3.0	54	7	5	-22	225	-104	18	1.20
21	3.3	54	8	5	-22	225	-104	12	1.20
22	3.3	55	8	5	-13	225	-89	12	1.20

Sigma-Aldrich (Steinheim, Germany); and 2-*n*-propylresorcinol (CAS Registry No. 13331-19-6) and 2-methylresorcinol (CAS Registry No. 608-25-3) were purchased from Alfa Aesar (Karlsruhe, Germany). Methanol of LC-MS grade (Fluka Chromasolv) was purchased from Sigma-Aldrich, and water was prepared on a Milli-Q Gradient A10 system by Millipore (Schwalbach, Germany).

The procyanidin B3 was synthesized following the method published by Delcour et al. and purified on a Sephadex LH-20 column.¹⁵ The required taxifolin (CAS Registry No. 480-18-2) was purchased from Foxtank GmbH (Berlin, Germany), and (+)-catechin (CA) (CAS Registry No. 154-23-4) was purchased from Sigma-Aldrich. (-)-epicatechin (EC) (CAS Registry No. 490-46-0) was purchased from Sigma-Aldrich. The synthesis of the methylated EC followed the procedure published by Donovan et al.¹⁶

The methylation of the hydroxy groups of 4-methylresorcinol and 4-methylpyrocatechol was performed according to the method published by Cren-Olive et al. with slight modifications.¹⁷

The identity of all synthesized substances was controlled via accurate mass determination, ¹H and ¹³C NMR solved in acetone-*d*₆ for 16–19 or in CDCl₃ for 11–14. In addition to ¹H and ¹³C experiments, heteronuclear single-quantum coherence (HSQC), heteronuclear multiple-bond correlation (HMBC), and 1D-difference nuclear Overhauser effect experiments have been performed for structure elucidation of the substances. The results fit to calculated masses and the NMR data found in the literature.

FTMS Parameters. All analyses were performed on a LTQ Orbitrap XL (Thermo Scientific, Bremen, Germany) and the collected data were evaluated with Xcalibur 2.07 software (Thermo Scientific). For syringe infusion the integrated syringe pump of the LTQ was used with a Hamilton gastight 1750 syringe fitted.

Before each measurement, the system was calibrated according to the LTQ Orbitrap XL manual. The deviation of the mass accuracy was 1.5 ppm or below.

The substances were either solved in methanol/water (1:1, v/v) (compounds 15–22) or for the less polar compounds in methanol/water (8:2, v/v) (compounds 1–14). Stock solutions with a concentration of 500 µg/mL were prepared. The concentrations for the measurement ranged from 5 to 100 µg/mL depending on the signal intensities. It was the goal to get signals with a minimum intensity of 10⁴, but before a higher concentrated solution was used,

the speed of the syringe pump was increased. Starting at 5 µL/min, it was raised to 15 µL/min to increase the signal intensity.

For every experiment an average spectrum of 30 s of measurement time was collected. The samples were measured until clear spectra were obtained; for larger molecules the number of repetitions was larger than for small molecules with less complex structures. During the experiments the most intense signals were selected manually. Fragment ions, which seemed important in comparison to spectra of other substances, were manually selected for further experiments whenever their intensity allowed it.

The manual selection during the syringe pump experiments is rather time-consuming compared to automated signal selection; however, the advantage of the manual method is that signals from the noise are not able to trigger experiments and deliver false data. Therefore, we decided to use manual selection exclusively.

The experiments were carried out in the negative ionization mode because for this ionization mode several typical neutral losses have been described in the literature. Examples for neutral losses are CO, CO₂, H₂O, or C₂H₂O.^{18,19} Other studies focused more on fragmentation pathways for polyphenolic compounds. Described are, for example, retro-Diels–Alder fission,²⁰ the quinone methide pathway,²¹ and heterocyclic ring fission.²²

The resolution was set to 60000 in FTMS mode. When the signal intensity for a fragment ion in the FTMS mode was not sufficient for further FTMS analysis, the ion trap (ITMS) was used for further fragmentation of this fragment ion. Therefore, for some fragment ions presented in this work FTMS data are not available. In Table 1 are summarized the FTMS parameters for all substances.

RESULTS AND DISCUSSION

To elucidate the mass spectrometric fragmentation pathway of polyphenols, a bottom-up approach using FTMS, starting with the small phenolic compounds 1–5 was chosen. In a first step, the impact of the substitution pattern on the product ion spectra of bishydroxylated benzenes was investigated. Fragmentation of compound 2, with ortho-positioned hydroxy functions, yielded a product ion spectrum with predominantly fragment ions resulting from the loss of H₂O (*m/z* 91.0193) and CO (*m/z* 81.0350). In contrast, for the fragmentation of 3,

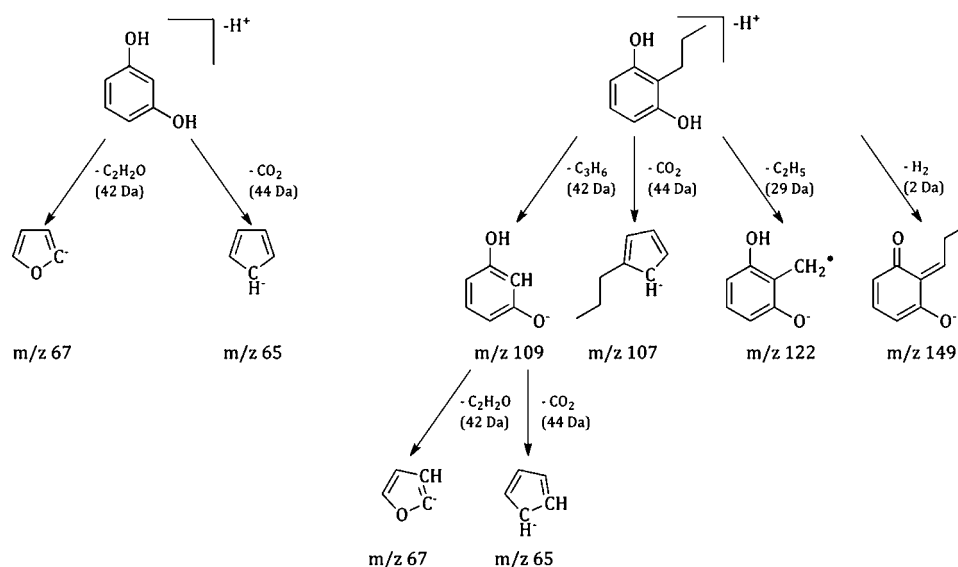


Figure 2. Fragmentation of **3** (left) and **10** (right) showing that an alkyl moiety attached to the benzene ring has no influence on the further fragmentation. The MS² experiments were carried out with FTMS, the MS³ with ITMS.

where the hydroxy functions are meta oriented, the loss of CO₂ (m/z 65.0401) was the largest fragment followed by the loss of C₂H₂O (m/z 67.0194) (see Supporting Figures 2 and 3 in the Supporting Information). The fragmentation of the para-configured compound **1** revealed a spectrum of generally low intensity with signals corresponding to the loss of CO₂ (m/z 65.0401) and CO (m/z 81.0350). Thus, all three compounds could clearly be differentiated due to different product ions formed as well as different relative signal intensities observed (see Supporting Figures 1–3 in the Supporting Information).

In a next step, the impact of a third hydroxy group was studied with compounds **4** and **5**.

In **4**, where the hydroxy groups are vicinal, the most intense fragment ion is caused by the cleavage of CO (m/z 97.0297), followed by a loss of CO₂ (m/z 81.0349) and H₂O (m/z 107.0140). No loss of C₂H₂O could be detected in the product ion spectrum of this compound. Fragmentation of **5**, a compound with all three hydroxy functions in the meta position, showed the loss of C₂H₂O (m/z 83.014) as the most intense signal.

Like compounds **1–3**, also **4** and **5** could clearly be differentiated due to their product ion spectra. Thus, generally, ortho-positioned hydroxy groups favor the loss of H₂O, whereas meta standing hydroxy groups support the loss of C₂H₂O in this set of model compounds.

To survey if moieties additionally attached to the benzene ring or to the hydroxy groups have further influence on the fragmentation pattern, compounds **6–14** have been analyzed by FTMS.

As an example for the observed spectral differences and analogies, the proposed fragmentation pathways of **3** and **10** are shown in Figure 2. In the case of **10** two strong signals, one standing for the loss of the propyl group (m/z 109.0298) and one for the loss of CO₂ (m/z 107.0868), were obtained. Additionally, two weaker signals resulting in modifications of the side chain could be observed. Following the loss of the propyl group, MS³ experiments of m/z 109.0298 revealed the nearly identical fragmentation pattern (see Figure 3) with m/z 67 (neutral loss of C₂H₂O) and m/z 65 (neutral loss of CO₂) as the strongest signals as found for **3**.

For smaller substituents such as methyl groups attached to the aromatic ring, no neutral loss but a radical cleavage of the aliphatic side chain can be observed. Nevertheless, as shown in Figure 4, also after the radical cleavage of the methyl group from **6**, similar MS³ fragments are formed as detected in the MS² spectrum of the nonsubstituted compound **2**. In both cases the fragment due to the loss of CO (–28 Da) is detected. The fragment for the loss of H₂O (–18 Da) could not be detected for **6** because of the low signal intensity.

In conclusion, these results show that an aliphatic group attached to the benzene ring has nearly no effect on subsequent fragmentation reactions performed after the loss of the respective group either by neutral loss or radical cleavage.

In addition to that, compounds **6–9** all show a neutral loss of 28.031 Da (identified as C₂H₄ with FTMS; see Supporting Figures 6–9 in the Supporting Information), which did not appear for **2** and **3**. This loss of C₂H₄ seems to be characteristic for small aliphatic groups attached to the aromatic ring of dihydroxy benzenes.

In the next step, methoxylated derivatives of **6** and **7** were analyzed to evaluate the impact of this modification on the fragmentation behavior. Compounds **6** and **7** were modified in a way that either one of the two hydroxy groups is methoxylated resulting in **11–14**. This modification is of special interest as such partially methylated polyphenols are possible metabolites of PA in organisms, for example, in pigs.²³ Also, it should help to verify if it is possible to distinguish between relatively similar compounds.

Compounds **11–14** all showed an altered fragmentation pattern compared to **6** and **7**. The most intense signal for **11–14** is the loss of a methyl group (–15.023 Da; m/z 122.0374; see Supporting Figures 11–14 in the Supporting Information). Further analysis of the spectra of **11–14** showed that, similar to **6–9**, a loss of C₂H₄ (28.031 Da) occurs, giving m/z 109.0298. Thus, no new specific fragments for the methoxylated derivatives could be observed.

Instead, ITMS MS³ experiments analysis of the fragment ion with m/z 122.0374 from **11–14** revealed that the fragmentation patterns for **11** and **12**, as well as those for **13** and **14**, are quite similar to the MS² spectra of the nonmethoxylated

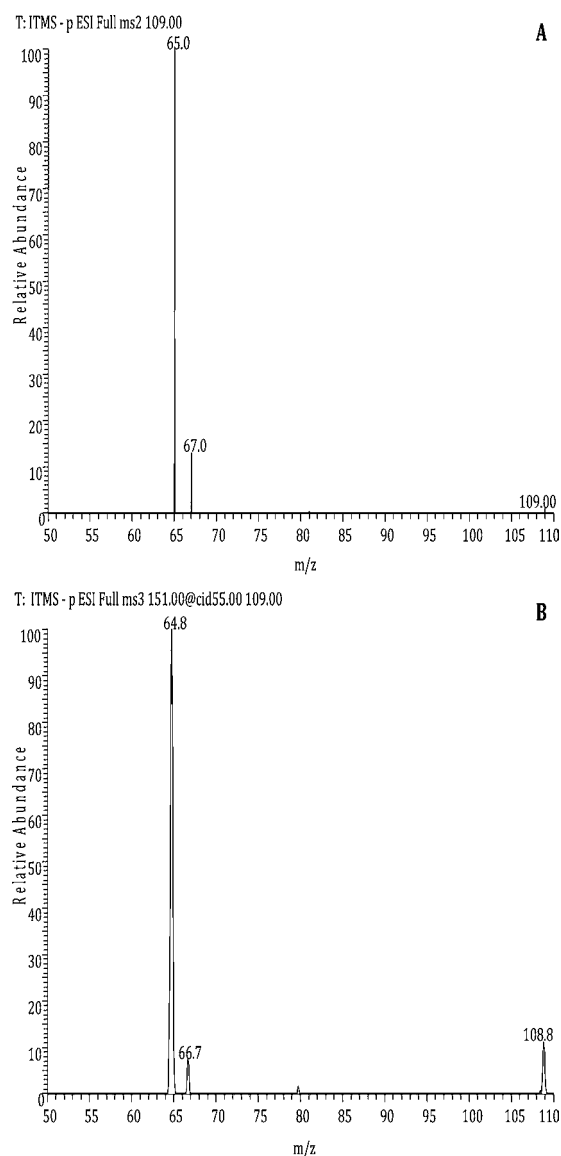


Figure 3. Comparison of the ITMS fragment spectra of **3** (A) and **10** (B). As shown for both compounds the same fragment ions are found.

compounds **6–9**. A detailed comparison of the MS³ spectrum of **12** with the MS² spectrum of **6** showed that the losses observed are quite identical (see Figure 5). After the loss of the methyl group from the methoxy group of **12**, the fragmentation pattern shows nearly the same fragment ions as the one gained from **6**. Especially the loss of 28 Da gave a strong signal, whereas further fragment ions of **12** could not be detected due to the low intensity of the signals. An important influence of the methoxylation is, however, that the characteristic neutral losses of H₂O for ortho-positioned hydroxy groups and of CO₂ for meta-positioned groups can no longer be observed and do not appear in MS³ after the radical cleavage of CH₃.

The final step of our project was to verify if the results of the analysis of the small compounds could be transferred to larger phenolic compounds, for example, (–)-EC (**15**) and (–)-EC with different hydroxy groups modified to methoxy groups (**16–19**).

The structure of **15** (Figure 1) shows a hydroxylation pattern on its A ring similar to that of **3** and on its B ring similar to that of **2**. On the basis of the fragmentations observed for these

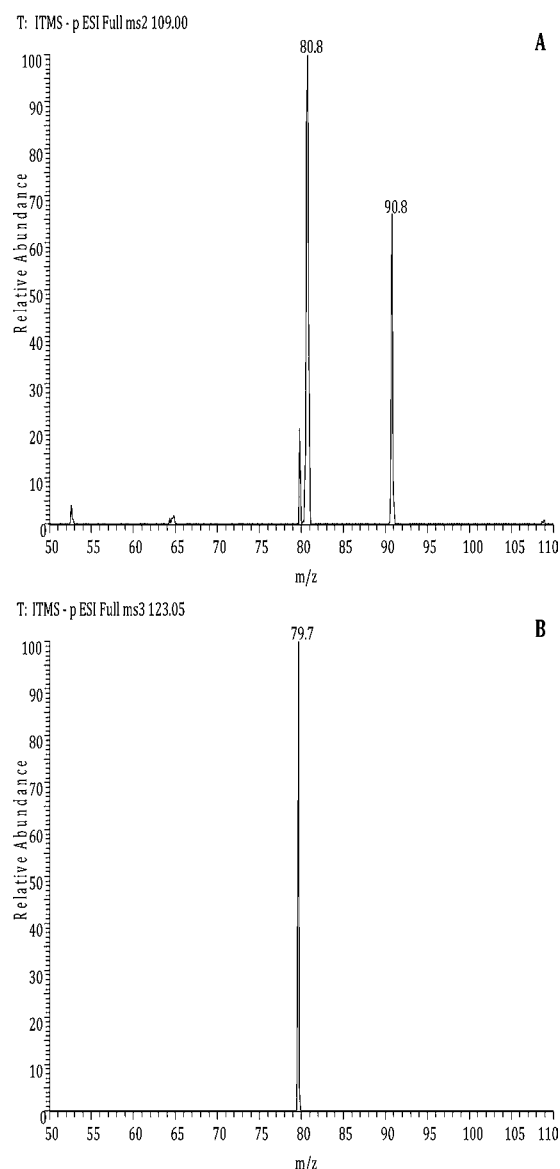


Figure 4. ITMS spectra of **2** (A) and **6** (B). The typical loss of CO (–28 Da) could be detected for **6** after the cleavage of the aliphatic methyl group.

model compounds, the MS² fragment spectrum of **15** was screened for corresponding losses of CO₂ and C₂H₂O (**3**), CO, and H₂O (**2**). In the MS² spectrum of **15**, fragment ions resulting from the loss of CO₂, C₂H₂O, and H₂O could be detected. However, to confirm the hypothesis that these fragmentation reactions of the model compounds can be transferred to **15**, methoxylated derivatives of **15** were analyzed.

As shown for **13** and **14**, a methoxylation of a hydroxy group inhibits the direct loss of CO₂ and C₂H₂O in MS² fragmentations. The losses of C₂H₂O and H₂O will be discussed later in this publication.

Thus, if the loss of CO₂ in **15** is caused from the A ring, a methoxylation of one of the hydroxy groups of this ring should also inhibit the loss of CO₂ from **18** and **19** as shown for **13** and **14**. For this reason the spectra of **18** and **19** were screened for the lack of a loss of CO₂ in the first step (see Figure 6). By comparing the intensity of the loss of CO₂ for **15** (to *m/z* 245.081) with **16** and **17** and with **18** and **19** (each to *m/z* 259.097), strong differences in the intensity of the respective

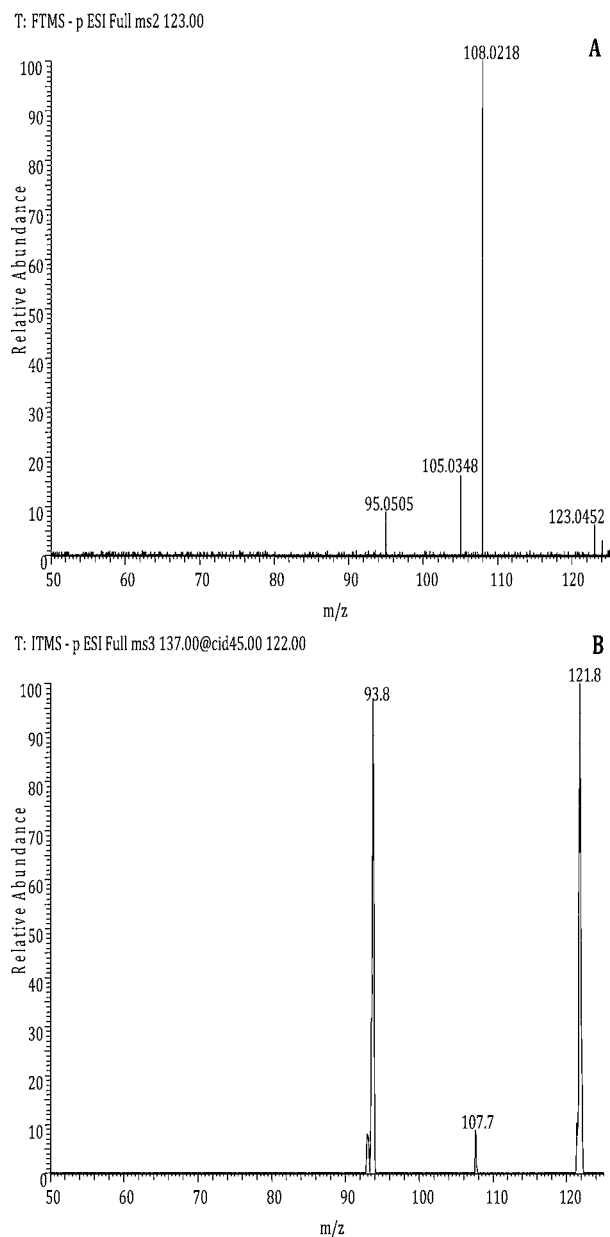


Figure 5. FTMS MS² spectrum of **6** (A) and ITMS MS³ spectrum of **12** (B). The loss of 28 Da (CO) could be detected for both compounds.

ion can be observed. Whereas for **15** this loss is the strongest one observed, with a relative intensity of 100%, and the loss is also quite strong for **16** and **17**, with relative intensities of about 65 and 50%, respectively, only traces of this fragment ion can be observed for **18** and **19** with a relative intensity of $\leq 1\%$ (all spectra are shown in the Supporting Information). In combination with the quinone methide fragmentation of polyphenols, a reaction in which oligomers are cleaved into their monomeric subunits during mass spectrometric fragmentation experiments,^{20,21} an identification of the hydroxylation pattern is possible even for larger molecules.¹⁰ The small traces of m/z 259.097 for **18** and **19** could be caused by an intramolecular rearrangement as cleavage and rearrangement reactions are competing reactions during CID experiments.²⁴ The possibility for rearrangements also might limit the applicability of this approach as each additional MS step

could also cause a rearrangement besides a cleavage reaction and thus a change in structure of some or even all fragment ions. An example for this is given later during the discussion of the fragmentation of EC in MS⁴ experiments. To get more information about the fate of the A ring, the spectrum of **20** was checked for losses of CO₂ and CO. A fragment ion with m/z 261.0764 (see Supporting Figure 20 in the Supporting Information) was found, which is due to the loss of CO₂, but no loss of CO was detectable. This information fits our hypothesis that the B ring is not involved in the first fragmentation step (MS² of **15**, see Figure 6). In a final step we checked if the hydroxy group of the C ring has any influence on the loss of CO₂. Therefore, **21** was screened for that neutral loss, and a correlating fragment ion with m/z 397.0926 was found. All of these results combined provide strong evidence that the neutral loss of CO₂ is originated in the A ring of **15** and its derivatives.

The loss of 42.010 Da, identified with FTMS as C₂H₂O (m/z 247.0608 for **15**; m/z 261.0767 for **16** and **17**), was observed with an intensity of 6% relative to the main fragment for **15**. The two neutral losses of CO₂ and C₂H₂O are also typical for **3**, which resembles the hydroxylation pattern of the A ring of **15–17**. The same neutral loss of C₂H₂O was identified with FTMS for **20** (m/z 263.0556), which also shows the same hydroxylation pattern as **3**, but not for **18** and **19**. These observations further support our idea that the B ring, in contrast to the A ring, is not part of the first fragmentation steps (MS² of, e.g., **15**) of the larger compounds **15–21**.

The above-mentioned neutral loss of H₂O, found for **15** (found together with neutral losses of CO₂ and C₂H₂O) and for model compound **2** in the MS² spectrum, was also detectable for **16–20**. The resulting fragment ions for **16–19** all showed a mass difference of 15.023 Da (CH₃ group). Therefore, we assume that the loss of H₂O does not originate from the B ring, although it shows the same hydroxylation pattern as **2**. Instead, we assume that the loss is a result of the fragmentation of the C ring. This fact, to our knowledge, so far has not been proven in experiments in which several compounds with similar hydroxylation patterns have been compared. This gives another strong hint that the fragmentation of larger substances such as **15** starts at the A ring and not at the B ring. The loss of H₂O found for **21** (see Supporting Figure 21 in the Supporting Information) could be a result of the fragmentation of the gallic acid moiety esterified to the hydroxy group of the C ring of the compound. The gallic acid moiety resembles the hydroxylation pattern found in **4**, which shows a loss of H₂O (see Supporting Figure 4 in the Supporting Information).

Finally, our finding that the B ring is not part of the MS² fragmentation path of **15** is additionally confirmed by the fact that we did not observe a loss of CO for **15–19** (see Supporting Figures 15–19 in the Supporting Information), which would be expected to be found in spectra gained from substances with the same hydroxylation pattern as in **2** and **6**.

The fragmentation of the B ring of **15** was investigated by further analysis of the fragment ion with m/z 245.0814 isolated after the loss of CO₂. A postulated structure of the fragment ion with m/z 245.0814 is shown in Figure 7. As described above, the loss of CO₂ was also detectable for **20** (m/z 261.0764), **21** (m/z 397.0926), and **16** and **17** (m/z 259.0971) as a result of the fragmentation of the A ring. As shown in Figure 7, the A ring no longer carries any hydroxy groups. From the fragment ion with m/z 245.0814 it was possible to generate a fragment

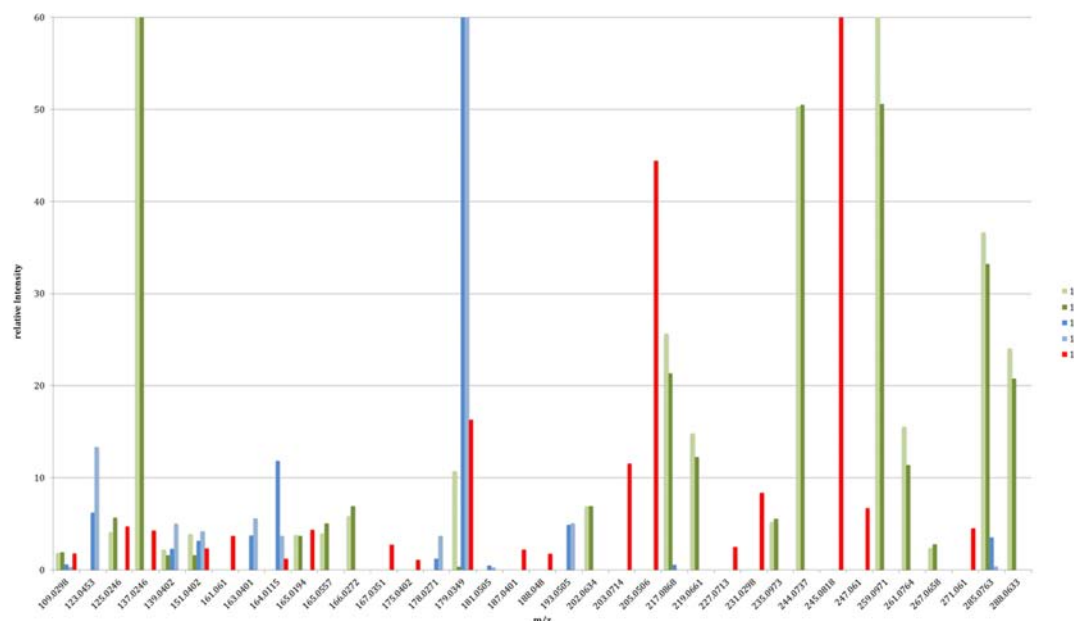


Figure 6. Relative intensities of the fragment ions obtained from the FTMS spectra of 15–19 compared to each other. The y-axis has been scaled to 60% for overview. However, the lack of losses of CO_2 and $\text{C}_2\text{H}_2\text{O}$ (m/z 261, corresponding m/z 247 from 15) from 18 and 19 are clearly visible, which in contrast can be seen for 16 and 17.

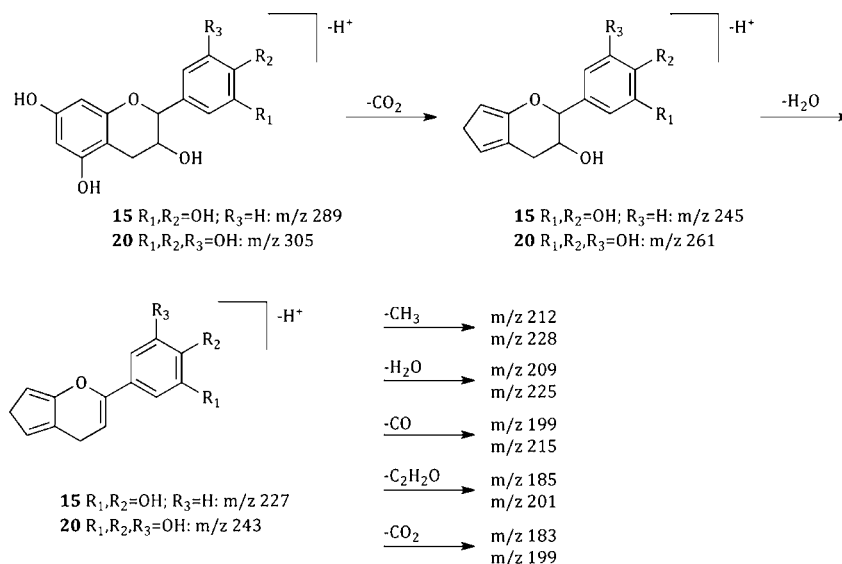


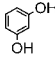
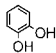
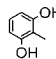
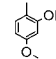
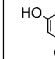
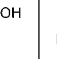
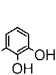
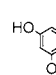
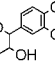
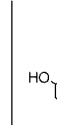
Figure 7. Postulated fragmentation path of 15 and 20 as an example for the elucidation of the fate of the B-ring. The difference between both fragment ions is equivalent to a hydroxy group.

ion with m/z 227.0712 (-18.010 Da). The neutral loss could be identified with FTMS as H_2O , which comes most likely from the C ring (see above). In the following MS experiments with the fragment ion m/z 227.0712 we found a fragment ion with m/z 212.0833 ($-\text{CH}_3$) with the highest intensity and a fragment ion with m/z 199.0763 ($-\text{CO}$; 38% of the signal intensity of m/z 212.0833). Losses of H_2O , $\text{C}_2\text{H}_2\text{O}$, and CO_2 with intensities $<10\%$ compared to m/z 212.0833 were also observed with FTMS. Due to our observations about the fragmentation of 2, we assume that the neutral losses of CO and H_2O were a result of the degradation of the B ring of 15. These results are supported by the fact that the ITMS spectrum of 20 after a neutral loss of CO_2 followed by a neutral loss of H_2O gives a very similar fragmentation pattern with signals at m/z 228, 225, 215, 201, and 199.

The loss of CO_2 at this stage of the fragmentation was not expected and could best be explained by previous rearrangements. The loss of CO_2 was also found for 18 and 19 (see Supporting Figures 18 and 19 in the Supporting Information) with a low relative intensity ($<0.5\%$ compared to m/z 179.0349), where it should not occur because of the methoxy group on the A ring (compare 13 and 14). This loss of CO_2 might appear at this stage of the fragmentation due to the fact that these fragment ions were gained from MS^4 experiments where the internal energy and structure of the precursor ion may allow this unexpected loss of CO_2 .

The result of the described MS experiments proved that it is possible to identify specific structural elements of PC by their characteristic mass spectrometric fragmentation. The hydroxylation pattern has a huge influence on the fragmentation

Table 2. Overview over Neutral Losses Observed in Small Phenolic Compounds Which Can Also Be Detected in Larger Molecules, as long as the Structural Requirements for the Loss Are Met^a

										
	3	2	8	14	5	4	15	16	18	22
CO ₂	+	-	+	-	-	+	+	+	+	+
H ₂ O	-	+	-	-	-	+	+ ¹⁾	-	-	+
CO	-	+	-	-	-	-	-	-	-	-
CH ₃	-	-	+	+	-	-	-	+	+	-
C ₂ H ₂ O	+	-	+	-	+	-	+ ¹⁾	+	-	-
C ₃ O ₂	-	-	-	-	+	-	+ ¹⁾	+ ¹⁾	-	-
HRF	n.a.	n.a.	n.a.	n.a.	n.a.	n.a.	+	+	+ ²⁾	+
RDA	n.a.	n.a.	n.a.	n.a.	n.a.	n.a.	+	+ ³⁾	+	+
C ₆ H ₆ O ₂ (B-ring)	n.a.	n.a.	n.a.	n.a.	n.a.	n.a.	+	+ ⁴⁾	+	+

^aTo take into account that the loss of H₂O may be from the hydroxy groups of an aromatic ring or from the hydroxy group of the C-ring, two sequent losses of H₂O were monitored. Only substances where the meta-positioned hydroxy groups are present showed the second loss. The loss of CO₂, for example, can occur only if two hydroxy groups are occurring in meta-position. As soon as one of these groups is blocked by methoxylation, loss of CO₂ can no longer be observed. In a few cases some typical fragmentations can only be observed in MS³ or later because other fragmentations are much more dominant and, therefore, relative signal intensities are too weak. However, analysis for the typical neutral losses was carried out using precursors of fragmentation reactions occurring on other parts of the molecules, thus preventing an influence by previous fragmentations. HRF, heterocyclic ring fission (loss of phloroglucinol); RDA, retro-Diels–Alder reaction; n.a., not applicable. ¹⁾Second loss of H₂O considering a presumable loss from the C-ring ²⁾Loss of C₇H₈O₃ instead of C₆H₆O₃. ³⁾Loss of C₉H₁₀O₃ instead of C₈H₈O₃. ⁴⁾Loss of C₇H₈O₂ instead of C₆H₆O₂.

Table 3. Fragmentation Pattern of Compound 22 Compared with 15^a

(-)-epicatechin (15)	245.0871	231.0299	205.0506	179.0351	165.0196	151	137.0247
PC B3 (22)	245.0812	231	205.0502	179.0346	165	151	137

^aThe fragment ions of 22 were gained after isolation and further fragmentation of m/z 289 from m/z 577 [M - H]⁻. It is obvious that m/z 289 gained from 22 behaves like the parent ion of 15. Fragment ions without decimal places have been gained with ITMS due to their low intensity.

behavior of the substances analyzed in this study. We were able to apply the results of the analysis of smaller phenolic compounds to the larger (-)-EC (15) and its derivatives, which show a hydroxylation pattern like that of the small phenolic compounds, for example, 2 and 3.

In their recent publication van der Hooft et al. showed specific fragment ions for larger phenolic compounds.²⁵ We compared the data of epigallocatechin and epicatechin provided by van der Hooft in their Supporting Information with our own data. For the MS² experiments we found all of the given fragment ions and some additional ones. For epigallocatechin the same applies for the MS³ data with some minor differences. In the case of epicatechin, two of the three MS³ data sets did not match. The fragment ions C₁₅H₁₄O₆ and C₁₁H₇O₃ were not detected in our experiments. The reason for this might be very low signal intensities, and therefore the signals were considered as noise. Another explanation might be the fact that van der Hooft et al. used automatic signal selection in combination with a Xcalibur software feature called “dynamic exclusion list”. In a personal communication van der Hooft explained that very weak signals might have been isolated and further fragmented if the more intense signals were set on the dynamic exclusion list. So even the noise could trigger an MSⁿ experiment, and therefore we were not able to reproduce these results. Besides this, the reproducibility of the fragmentation is clearly given.

Modifications of the hydroxy groups, as used here in the form of methoxy groups to simulate metabolism or to simulate an ether bond found for A-type PC, create different spectra from the unaltered substances. This effect was observed for both the small phenolic compounds and the larger PC. The

observed effect seems to be limited to the fragmentation behavior of the ring to which the altered hydroxy groups are attached. This can be seen in the investigation of the fate of the B ring of (-)-EC (15), where a methoxy group attached to the B ring (as for 16 and 17) has no influence on the fragmentation of the A ring.

In Table 2 a summary of the fragmentation of some substances is shown. It is clearly visible that the hydroxylation pattern has a huge influence on the fragmentation. Also, the effect of methoxylation of a hydroxy group is shown again. It clearly blocks the neutral losses known from the unmodified compounds.

Nevertheless, it is also possible to preserve structural information from the spectra of these substances. Again we compared our data for 22 with the data by van der Hooft et al. for the same substance.²⁵ As for 15 and 20 the major fragment ions were matched, but due to our manual selection approach, some different ions were also detected. Nevertheless, the identification of oligomeric PC should not be a problem. To get more information about the structure of the compound, further fragmentation up to MS⁴ is necessary.

From our own experiments with oligomeric PC, for example, B3 (22), and from literature data we know that these substances are fragmented (compare Supporting Figure 22 in the Supporting Information) by MS into their monomeric components.^{26,27} These monomeric fragment ions can be further fragmented, and the resulting spectra are comparable to the ones gained directly from monomeric substances (Table 3).

With this information it should be possible to determine if an unknown compound carries the characteristic hydroxylation

pattern similar to that of the small phenolic compounds 1–3 or if one of the hydroxy groups is altered during metabolism and therefore specific neutral losses are prevented as shown for 16–19. In the literature van der Hooft et al. showed recently, that for, for example, morin and quercetin and several other isomeric compounds the hydroxylation pattern has a huge influence on the fragmentation pattern.¹⁴ Our work points out that even the smallest possible structure shows already a distinguishable fragmentation pattern. Therefore, it should be possible to search for these specific neutral losses found on the smallest compounds to get an idea about the structure of even larger molecules.

■ ASSOCIATED CONTENT

Supporting Information

Additional figures. This material is available free of charge via the Internet at <http://pubs.acs.org>.

■ AUTHOR INFORMATION

Corresponding Author

*Phone: +49 251 8333391. Fax: +49 251 8333396. E-mail: humpf@wwu.de.

Notes

The authors declare no competing financial interest.

■ REFERENCES

- (1) Rzeppa, S.; Von Barga, C.; Bittner, K.; Humpf, H. U. Analysis of flavan-3-ols and procyanidins in food samples by reversed phase high-performance liquid chromatography coupled to electrospray ionization tandem mass spectrometry (RP-HPLC-ESI-MS/MS). *J. Agric. Food Chem.* **2011**, *59*, 10594–10603.
- (2) Hellström, J. K.; Törrönen, A. R.; Mattila, P. H. Proanthocyanidins in common food products of plant origin. *J. Agric. Food Chem.* **2009**, *57*, 7899–7906.
- (3) Gu, L.; Kelm, M. A.; Hammerstone, J. F.; Beecher, G.; Holden, J.; Haytowitz, D.; Gebhardt, S.; Prior, R. L. Concentration of proanthocyanidins in common foods and estimation of normal consumption. *J. Nutr.* **2003**, *613*–617.
- (4) Porter, L. J. Flavans and proanthocyanidins. In *The Flavanoids – Advances in Research since 1986*; Harborne, J. B., Ed.; Chapman and Hall: London, UK, 1994; p 23 ff.
- (5) Rice-Evans, C. A.; Miller, N. J.; Paganga, G. Structure-antioxidant activity relationships of flavonoids and phenolic acids. *Free Radical Biol. Med.* **1996**, *20*, 933–956.
- (6) Koga, T.; Moro, K.; Nakamori, K.; Yamakoshi, J.; Hosoyama, H.; Kataoka, S.; Ariga, T. Increase of antioxidative potential of rat plasma by oral administration of proanthocyanidin-rich extract from grape seeds. *J. Agric. Food Chem.* **1999**, *47*, 1892–1897.
- (7) Miura, T.; Chiba, M.; Kasai, K.; Nozaka, H.; Nakamura, T.; Shoji, T.; Kanda, T.; Ohtake, Y.; Sato, T. Apple procyanidins induce tumor cell apoptosis through mitochondrial pathway activation of caspase-3. *Carcinogenesis* **2008**, *29*, 585–593.
- (8) Rasmussen, S. E.; Frederiksen, H.; Struntze Krogholm, K.; Poulsen, L. Dietary proanthocyanidins: occurrence, dietary intake, bioavailability, and protection against cardiovascular disease. *Mol. Nutr. Food Res.* **2005**, *49*, 159–174.
- (9) Shimada, T. Salivary proteins as a defense against dietary tannins. *J. Chem. Ecol.* **2006**, *32*, 1149–1163.
- (10) Engemann, A.; Hübner, F.; Rzeppa, S.; Humpf, H.-U. Intestinal metabolism of two a-type procyanidins using the pig cecum model: detailed structure elucidation of unknown catabolites with Fourier transform mass spectrometry (FTMS). *J. Agric. Food Chem.* **2012**, *60*, 749–757.
- (11) van't Slot, G.; Mattern, W.; Rzeppa, S.; Grewe, D.; Humpf, H.-U. Complex flavonoids in cocoa: synthesis and degradation by intestinal microbiota. *J. Agric. Food Chem.* **2010**, *58*, 8879–8886.
- (12) Vallverdu-Queralt, A.; Jauregui, O.; Medina-Remon, A.; Andres-Lacueva, C.; Lamuela-Raventos, R. M. Improved characterization of tomato polyphenols using liquid chromatography/electrospray ionization linear ion trap quadrupole Orbitrap mass spectrometry and liquid chromatography/electrospray ionization tandem mass spectrometry. *Rapid Commun. Mass Spectrom.* **2010**, *24*, 2986–2992.
- (13) Kerwin, J. L. Negative ion electrospray mass spectrometry of polyphenols, catecholamines and their oxidation products. *J. Mass Spectrom.* **1996**, *31*, 1429–1439.
- (14) van der Hooft, J. J. J.; Vervoort, J.; Bino, R. J.; Beekwilder, J.; de Vos, R. C. H. Polyphenol identification based on systematic and robust high-resolution accurate mass spectrometry fragmentation. *Anal. Chem.* **2011**, *83*, 409–416.
- (15) Delcour, J. A.; Ferreira, D.; Roux, D. G. Synthesis of condensed tannins. Part 9. The condensation sequence of leucocyanidin with (+)-catechin and with the resultant procyanidins. *J. Chem. Soc., Perkin Trans. 1* **1983**, 1711–1717.
- (16) Donovan, J. L.; Luthria, D. L.; Stremple, P.; Waterhouse, A. L. Analysis of (+)-catechin, (–)-epicatechin and their 3'- and 4'-O-methylated analogs a comparison of sensitive methods. *J. Chromatogr., B: Biomed. Sci. Appl.* **1999**, *726*, 277–283.
- (17) Cren-Olive, C.; Lebrun, S.; Hapiot, P.; Pinson, J.; Rolando, C. Selective protection of catechin gives access to the intrinsic reactivity of the two phenol rings during H-abstraction and photo-oxidation. *Tetrahedron Lett.* **2000**, *41*, 5847–5851.
- (18) Fabre, N.; Rustan, I.; de Hoffmann, E.; Quetin-Leclercq, J. Determination of flavone, flavonol, and flavanone aglycones by negative ion liquid chromatography electrospray ion trap mass spectrometry. *J. Am. Soc. Mass Spectrom.* **2001**, *12*, 707–715.
- (19) McNab, H.; Ferreira, E. S. B.; Hulme, A. N.; Quye, A. Negative ion ESI-MS analysis of natural yellow dye flavonoids – an isotopic labelling study. *Int. J. Mass Spectrom.* **2009**, *284*, 57–65.
- (20) Friedrich, W.; Eberhardt, A.; Galensa, R. Investigation of proanthocyanidins by HPLC with electrospray ionization mass spectrometry. *Eur. Food Res. Technol.* **2000**, *11*, 56–64.
- (21) Karchesy, J. J.; Foo, L. Y.; Barofsky, E.; Arbogast, B.; Barofsky, D. F. Negative-ion fast-atom-bombardment mass spectrometry of procyanidin oligomers. *J. Wood Chem. Technol.* **1989**, *9*, 313–331.
- (22) Li, H.-J.; Deinzer, M. L. Tandem mass spectrometry for sequencing proanthocyanidins. *Anal. Chem.* **2007**, *79*, 1739–1748.
- (23) Rzeppa, S.; Bittner, K.; Döll, S.; Dänicke, S.; Humpf, H. U. Urinary excretion and metabolism of procyanidins in pigs. *Mol. Nutr. Food Res.* **2012**, *56*, 653–665.
- (24) Gabelica, V.; De Pauw, E. Internal energy and fragmentation of ions produced in electrospray sources. *Mass Spectrom. Rev.* **2005**, *24*, 566–587.
- (25) van der Hooft, J. J.; Akermi, M.; Unlu, F. Y.; Mihaleva, V.; Roldan, V. G.; Bino, R. J.; de Vos, R. C.; Vervoort, J. Structural annotation and elucidation of conjugated phenolic compounds in black, green, and white tea extracts. *J. Agric. Food Chem.* **2012**, *60*, 8841–8850.
- (26) de Souza, L. M.; Cipriani, T. R.; Iacomini, M.; Gorin, P. A. J.; Sasaki, G. L. HPLC/ESI-MS and NMR analysis of flavonoids and tannins in bioactive extract from leaves of *Maytenus ilicifolia*. *J. Pharm. Biomed. Anal.* **2008**, *47*, 59–67.
- (27) Sun, W.; Miller, J. M. Tandem mass spectrometry of the B-type procyanidins in wine and B-type dehydrodiccatechins in an autoxidation mixture of (+)-catechin and (–)-epicatechin. *J. Mass Spectrom.* **2003**, *38*, 438–446.